Biochemical and Biophysical Research Communications 458 (2015) 411–417

Contents lists available at ScienceDirect

Biochemical and Biophysical Research Communications

journal homepage: www.elsevier.com/locate/ybbrc

Activation of autophagy in response to nanosecond pulsed electric field exposure

Jody C. Ullery [a, *], Melissa Tarango [a], Caleb C. Roth [b], Bennett L. Ibey [c]

[a] General Dynamics Information Technology, JBSA Fort Sam Houston, TX, USA
[b] School of Medicine, Department of Radiological Sciences, University of Texas Health Science Center San Antonio, San Antonio, TX 78229, USA
[c] Air Force Research Laboratory, 711th Human Performance Wing, Human Effectiveness Directorate, Bioeffects Division, Radio Frequency Bioeffects Branch, JBSA Fort Sam Houston, TX, USA

ARTICLE INFO

Article history:
Received 12 January 2015
Available online 7 February 2015

Keywords:
Nanosecond electric pulse
Autophagy
CHO

ABSTRACT

Previous work demonstrated significant changes in cellular membranes following exposure of cells to nanosecond pulsed electric fields (nsPEF), including nanoporation and increases in intracellular calcium concentration. While it is known that nsPEF exposure can cause cell death, how cells repair and survive nsPEF-induced cellular damage is not well understood. In this paper, we investigated whether autophagy is stimulated following nsPEF exposure to repair damaged membranes, proteins, and/or organelles in a pro-survival response. We hypothesized that autophagy is activated to repair nsPEF-induced plasma membrane damage and overwhelming this compensatory mechanism results in cell death. Activation of autophagy and subsequent cell death pathways were assessed measuring toxicity, gene and protein expression of autophagy markers, and by monitoring autophagosome formation and maturation using fluorescent microscopy. Results show that autophagy is activated at subtoxic nsPEF doses, as a compensatory mechanism to repair membrane damage. However, prolonged exposure results in increased cell death and a concomitant decrease in autophagic markers. These results suggest that cells take an active role in membrane repair, through autophagy, following exposure to nsPEF.

1. Introduction

Exposure of cells to nanosecond pulsed electric fields (nsPEF) leads to the formation of plasma membrane pores approximately 1–2 nm in diameter, referred to as nanopores [1–3]. Nanopores allow the passage of small ions through the plasma membrane and can contribute to cell death mechanisms [4]. In addition to nanoporation, exposure to nsPEF results in damage to cellular structures including the plasma membrane, cytoskeleton, and organelle membranes [5–7]. Such damage can lead to the activation of cell death pathways [7,8].

Autophagy is a cellular process that is activated as an adaptive response to a number of extracellular and intracellular stresses, including cellular membrane damage. Importantly, the activation of autophagy allows cells to reclaim critical amino acids and other metabolic building blocks, such as energy producing components from damaged organelles and membranes by delivering them to the lysosome for degradation and repurposing. While the initial objective of autophagy is cell survival and repair, autophagy may also facilitate an organized cell death [9]. Recent studies suggest autophagy may be activated in response to noninvasive radiofrequency (RF) treatment of tumors [6,10–12]. However, extensive studies to determine the relationship between nsPEF exposure and autophagic mechanisms have not been performed.

In this study, we aim to establish the link between nsPEF exposure and the temporal activation of autophagy by varying the duration of nsPEF exposure (i.e., number of pulses) and measuring cellular effects over time. Activation of autophagy and subsequent cell death pathways are assessed by examining the cellular response to nsPEF exposure, including measuring toxicity markers, gene and protein expression of autophagy markers, and immunofluorescent tracing of autophagosome formation and maturation. We hypothesize that autophagy is activated to repair nsPEF-induced plasma membrane damage (Fig. 1A). We postulate that when cellular damage is over a certain nsPEF exposure threshold, cell death ensues. Therefore, we hypothesize that continual

* Corresponding author. General Dynamics Information Technology, 4141 Petroleum Road, Bldg. 3260, JBSA Fort Sam Houston, TX 78234, USA. Fax: +1 210 539 7945.
E-mail address: jody.ullery.ctr@us.af.mil (J.C. Ullery).

http://dx.doi.org/10.1016/j.bbrc.2015.01.131
0006-291X/

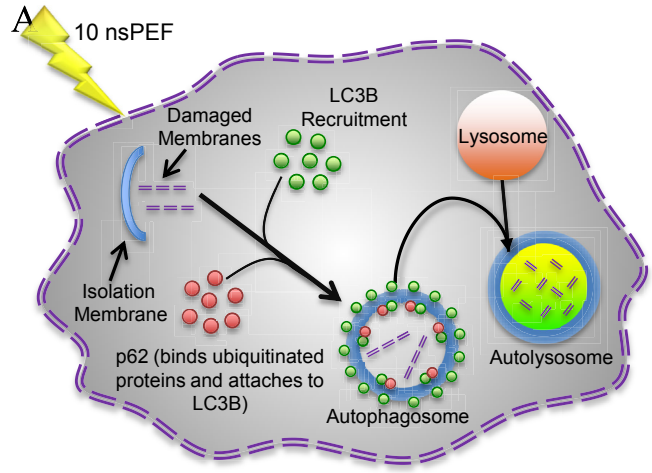

B

UniGene ID:	Hs.529892
Accession No:	NM_003900
Gene Name:	Sequestome 1
Symbol:	SQSTM1
Fold change 150kV vs. SHAM:	3.044

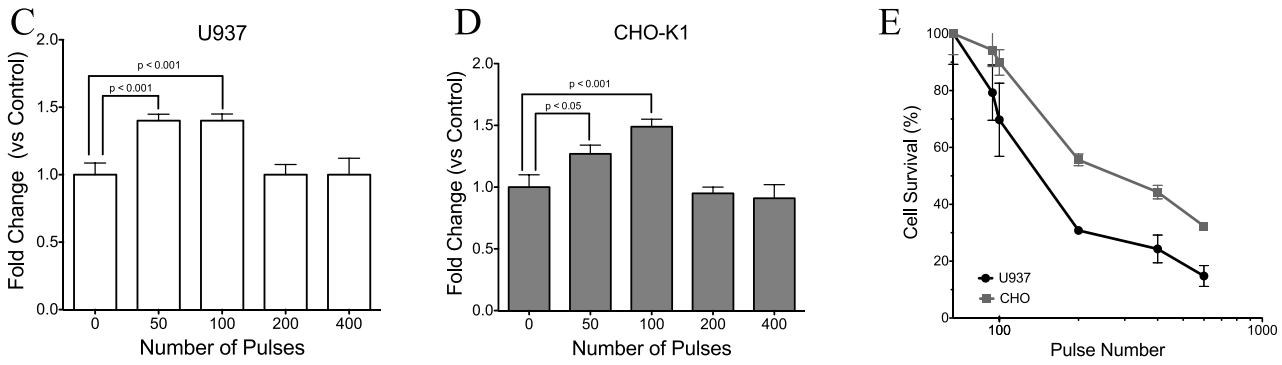

Fig. 1. Changes in p62 gene expression levels following nsPEF exposure and relationship to cell death. (A) Simplified model of the hypothesis tested within this manuscript, which addresses the activation of autophagy in response to nsPEF exposure. (B) Alteration in sequestome 1 (SQSTM1 or p62) gene expression in U937 by microarray analysis at 4 h post nsPEF exposure. Cells were pulsed at 150 kv/cm for 100 pulses and compared to sham (untreated) cells. (C) Consistent with microarray results, we observe an increase in p62 gene expression at low pulse numbers (50 and 100) in U937 cells. (D) The increase in p62 does not appear to be cell-type specific, as we observe a similar increase in gene expression in CHO-K1 cells. (E) Cell survival was assessed by MTT cell viability assay, for comparison to expression data.

exposure to nsPEF results in cell death by overwhelming this compensatory mechanism.

2. Materials and methods

2.1. Cell culture and 10 nsEP exposure

U937 human monocyte and Chinese Hamster Ovarian-K1 (CHO-K1) cell lines were obtained from ATCC (Manassas, VA). U937 monocytes were cultured in RPMI-1640 medium supplemented with 10% fetal bovine serum, 2 mM L-glutamine, and 100 U/mL penicillin/streptomycin. CHO-K1 cells were cultured in F12K medium supplemented with 10% fetal bovine serum, 2 mM L-glutamine, and 100 U/mL penicillin/streptomycin at 37 °C with 5% CO_2 in air. The media and its components were purchased from ATCC (Manassas, VA).

Cells were exposed to 10 nsPEF as described previously [13]. U937 cells were centrifuged and re-suspended in fresh medium at a density of 1200 cells/μL. CHO-K1 cells were removed from the culture dish with 0.25% Trypsin-EDTA (ATCC) and suspended in fresh, serum free F12K medium at a density of 1200 cells/μL. Cells (140 μL) were exposed to 10 ns pulses in a conventional electroporation cuvette with a 1-mm gap (BioSmith Biotech, San Diego, CA) for 50 to 600 pulses at an amplitude of 150 kV/cm and a 1 Hz repetition rate. Nearly rectangular pulses of 10-ns width were produced by a Blumlein line generator. To produce nsEP, the Blumlein line was charged from a high-voltage DC power supply (Glassman High Voltage Inc, High Bridge, NJ) until a breakdown voltage was reached across a spark gap in a pressurized switch chamber. The breakdown voltage was varied from 15 to 25 kV by changing the pressure of SF_6 gas in the switch chamber. The amplitude, number of pulses, and pulse shape of nsEP delivered to the sample were continuously monitored on a 2.5 GHz digital oscilloscope (DSO9254A, Agilent Technologies, Cedar Creek, TX) via a custom-made high-voltage probe. All exposures were performed at room temperature.

2.2. MTT cell viability assay

At 24 h post-exposure, cell survival was assessed using an MTT Cell Proliferation Assay (3-(4, 5-Dimethylthiazol-2-yl)-2,5-diphenyltetrazolium bromide, (ATCC, Manassas, VA) according to the manufacturer's protocol. Briefly, 30 μL of exposed cells were aseptically aliquoted to 96-well dishes in triplicate to wells containing 70 μL of fresh media, and incubated at 37 °C for 24 h. Following incubation, 10 μL MTT reagent was added and returned to a 37 °C incubator for 2 h until precipitate was visible. 100 μL of detergent was added to each well, and the plate was stored in the dark at room temperature overnight. The following day, absorbance was measured at 570 nm with a Synergy HT Microplate Reader (BioTEK, Winooski, VT), and the readings were normalized to untreated controls.

2.3. Microarray and microarray data analysis

Expression analysis was performed for each time point in triplicate (three control and three nsEP exposed) using the Affymetrix GeneChip® Human Genome U133 (HG-U133) plus 2.0 Array that contains 54,675 probe sets. Briefly, two micrograms of RNA were used for preparation of biotin-labeled targets (cRNA) using MessageAmp™-based protocols (Ambion, Inc., Austin, TX). Labeled cRNA was fragmented (0.5 μg/μL per reaction) and was used for array hybridization and washing. The cRNA was mixed with a hybridization cocktail, heated to 99 °C for 5 min and then incubated at 45 °C for 5 min. Hybridization arrays were conducted for 16 h in an Affymetrix Model 640 hybridization oven (45 °C, 60 rpm). Arrays were washed and stained on an FS450 Fluidics station and were scanned on a GeneChip® Scanner 3000 7G. Image signal data, detection calls and annotations were generated for every gene using the Affymetrix Statistical Algorithm MAS 5.0 (GeneChip® Operating Software v1.3). A log2 transformation was conducted and a Student's t-test was performed for comparison of the two groups (control and nsEP exposed). We conducted multiple testing correction—Benjamini and Hochberg—to determine the false discovery rate, and statistical significant genes were identified using Bonferroni correction procedures ($-\log10$ pcutoff > 6.04).

For interpretation of the results, the Ingenuity Pathways Analysis tool (IPA version 8.7, Ingenuity® Systems Inc., Redwood City, CA; www.qiagen.com/ingenuity) was used. IPA is a web-based software application, which enables filtering and dataset comparisons, to identify biological mechanisms, pathways, and functions most relevant to experimental datasets or differentially expressed genes. The cut-off criteria for our IPA analysis were: an absolute value of log2 ratio $\geq$1.95 and a p-value $\leq$0.05. Other web-based resources, such as the GeneCards Human Gene Database, the HUGO Gene Nomenclature Committee (HGNC), and Gene Ontology were also used to further supplement the analysis.

2.4. Quantitative RT-PCR

At 4 and 16 h post-exposure, mRNA was isolated from pulsed and sham cells using the RNeasy RNA Collection Kit (Qiagen, Valencia, CA), following the manufacturer's instructions. RNA concentration was measured on a NanoDrop spectrophotometer (NanoDrop Technologies, Wilmington, DE). Total RNA (1 μg) was used in each reverse transcription reaction with the Verso cDNA kit, according to manufacturer's instructions (Thermo Scientific, Rockford, IL). One-tenth of each reaction volume (2 μl) was used per well in subsequent real time PCR analysis using TaqMan® Gene Expression Master Mix Kit (Applied Biosystems, Foster City, CA). Real time reactions were performed using a StepOnePlus Real Time PCR System running StepOne Software v2.1 (Applied Biosystems). Standard curves were generated by the amplification of target sequences that were previously cloned into pGEM-T (Promega, Madison, WI), in a dilution series from 10^{-1} to 10^{-6} fmol/well.

2.5. Western blotting

For total protein extraction, cell pellets were solubilized in cold TNE lysis buffer (50 mM Tris–HCl – pH 7.4, 100 mM NaCl, 0.1 mM EDTA) containing protease inhibitors (Sigma–Aldrich, St. Louis, MO). Protein lysates were cleared by centrifugation and stored at −20 °C. Protein concentrations were determined using a Bradford protein assay (Bio-Rad, Hercules, CA). For Western blotting, equal amounts of protein were resolved by electrophoresis on a 4–20% SDS-PAGE gel, transferred onto 0.2-μm PVDF membrane, and incubated in blocking buffer prior to the addition of primary antibodies. Following incubation with primary and secondary antibodies, luminol-based detection was performed using the SuperSignal West Dura Extended Duration Substrate Kit (Thermo Scientific). Primary and secondary antibodies were obtained from the following sources: p62 (Abcam, Cambridge, MA), beclin, Atg5, Atg12, LC3A/B-I, LC3A/B-II (Cell Signaling, Danvers, MA); goat anti-rabbit- and goat anti-mouse- IgG HRP (EMD Millipore, Temecula, CA).

2.6. Baculoviral transduction

CHO-K1 cells were transduced with Premo™ Autophagy Sensors LC3B-GFP and p62-RFP using BacMam 2.0 technology according to manufacturer's instructions (Molecular Probes Inc., Eugene, OR). Briefly, cells were collected and diluted to a final concentration of 4×10^5 cells in 2 mL of complete medium in T25 culture flasks (Falcon, Fisher Scientific, Houston, TX). To each suspension 120 μl of LC3B-GFP and p62-RFP reagent was added and cells were incubated at 37 °C for 24 h. Following transduction, cells were trypsinized and resuspended in complete medium at a final concentration of 1200 cells/μL and pulsed as described above. After pulsing, 140 μL of cells were then added to 2 mL of complete medium in a poly-D-lysine coated glass bottomed dish (MatTek Corp, Ashland, MA). Following a 16 h recovery period, we examined immunofluorescence using a Zeiss 710-LSM confocal microscope (Carl Zeiss MicroImaging, Thornwood, NY) and Zen 9.0 imaging software (Carl Zeiss MicroImaging, Thornwood, NY), as previously described [13].

2.7. Cyto-ID® immunostaining

In order to visualize autophagic vesicle formation in live cells, U937 cells or CHO-K1 cells were exposed to nsPEF as described above, plated in glass-bottomed dishes (MatTek Corp, Ashland, MA), and incubated at 37 °C for 18 h. Cells were rinsed twice with 1X phosphate buffered saline (PBS) and immunostained with Cyto-ID® Autophagy Detection reagent (Enzo Life Sciences, Farmingdale, NY) for 30 min at 37 °C. Following exposure, cells were rinsed twice more in 1X PBS and imaged as described above.

3. Results and discussion

3.1. Autophagy gene expression

Microarray studies were used to define global gene expression changes following nsPEF exposure in U937 cells. In combination with gene ontology, microarray studies were designed to identify specific pathways that may be affected by nsPEF exposure, including autophagy. Results show the up- or down-regulation of 335 genes of interest (data not shown). Among these, sequestome 1 (SQSTM1 or p62) was increased by over 3-fold when exposed to 10 nsPEF (150 kv/cm, 100 pulses) (Fig. 1B). Previous studies have shown that p62 is upregulated in response to increased cellular damage [14]. Specifically, p62 functions as an essential cargo adapter protein by binding ubiquitinylated, damaged cellular protein aggregates and mediating their autophagic degradation (Fig. 1A) [15–19].

In order to validate microarray data and pursue studies of nsPEF-induced autophagy, changes in p62 gene expression were analyzed by RT-PCR. Consistent with microarray data, there is an up-regulation of p62 expression at 50 and 100 pulses in U937 cells (Fig. 1C). However, p62 levels are not increased at higher pulse numbers in exposed U937 cells (Fig. 1C). p62 levels are also increased in CHO-K1 cells following 50 and 100 pulses (Fig. 1D). In contrast to U937 cells, elevated p62 is maintained at higher pulse numbers (Fig. 1D). Cell survival curves are shown to compare p62

upregulation to cell death (Fig. 1E). Results show a peak in p62 gene expression at 100 pulses for both U937 cells and CHO-K1 cells, which correlates to low levels of cellular toxicity, as measured by MTT cell viability (Fig. 1C–E).

3.2. p62 and LC3B are recruited to autophagosomes following nsPEF exposure

One of the earliest events of autophagy is the recruitment of p62 and LC3B to sites of autophagosome formation (Fig. 1A). Since we observe an elevation in p62 gene expression, we studied the formation of autophagosomes using the BacMam 2.0 viral transduction system to specifically label LC3B and p62 with GFP and RFP, respectively. U937 cells are resistant to viral transduction due to their hematopoietic origin [20]; therefore, CHO-K1 cells were used for this experiment. In non-stimulated (negative control) cells, the LC3B-GFP and p62-RFP immunostaining is diffuse (i.e., cytoplasmic), consistent with a lack of organized and active autophagosomes (Fig. 2, top row). However, with increased number of pulses, the LC3B-GFP and p62-RFP immunostaining becomes punctate and the colocalization becomes more pronounced with increasing pulse number (Fig. 2, rows 2–4). Importantly, the colocalization of LC3B-GFP and p62-RFP immunofluorescence suggests the recruitment of both proteins to developing autophagosomes. Chloroquine diphosphate (CQ), an inhibitor of late-stage autophagosome-lysosome fusion (leading to the accumulation of autophagosomes), is included as a positive control for autophagy induction (Fig. 2, bottom row).

3.3. Cyto-ID immunofluorecence

As the autophagic process develops, autophagosomes fuse with lysosomes to deliver their cargo for degradation (Fig. 1A). We utilized Cyto-ID® immunostaining to determine if nsPEF exposure

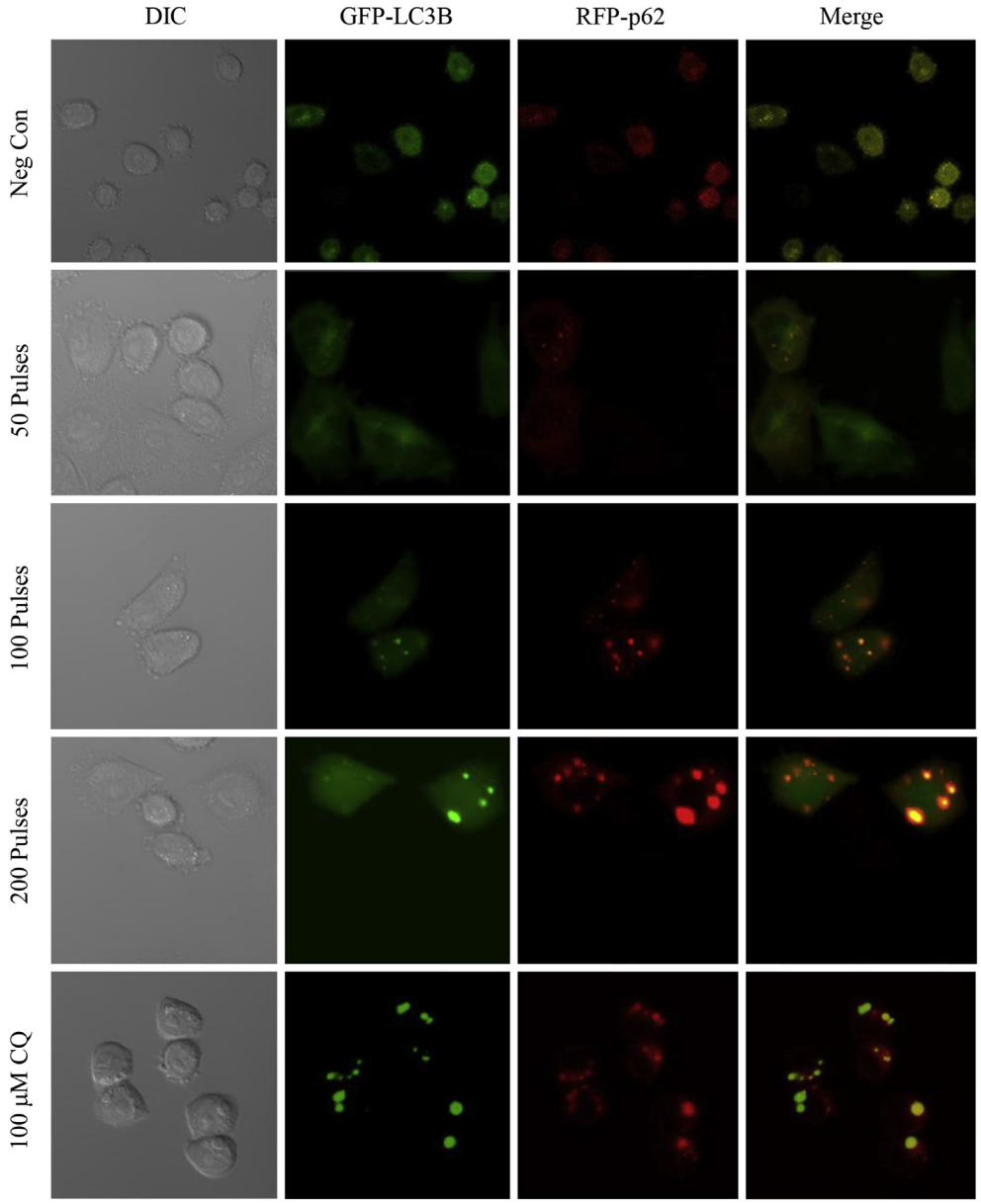

Fig. 2. nsPEF exposure induces LC3B and p62 recruitment to maturing autophagosomes. Unexposed cells maintain disperse (i.e. cytosolic) distribution (top row). As the number of nsPEF pulses increases, the increased fluorescence and colocalization of LC3B-GFP and p62-RFP suggests formation and maturation of autophagic vacuoles following nsPEF exposure (rows 2, 3, and 4). 100 μM chloroquine (CQ) is included as a positive control (bottom row).

results in mature autolysosome formation. The Cyto-ID® dye selectively labels autophagic vacuoles, allowing monitoring of autophagic flux in live cells [21]. We begin to observe Cyto-ID® staining of autophagic vesicles in U937 cells at 50 pulses and immunofluorescence gradually increases at 100 pulses (Fig. 3). Exposure of cells to 200 pulses results in a slight decrease in Cyto-ID® immunofluorescence in U937 cells (Fig. 3). The same trend is observed in pulsed CHO-K1 cells with a maximum Cyto-ID® immunofluorescence achieved at 200 pulses (Fig. 3). The mTOR inhibitor rapamycin was used as a positive control (Fig. 3, bottom row).

Importantly, Cyto-ID® immunostaining correlates to nsPEF toxicity. Specifically, Cyto-ID® immunostaining is highest at sub-lethal nsPEF exposures (Fig. 1E). Furthermore, the observed decrease in Cyto-ID®-stained vesicles occurs concurrently with increases in propidium iodide (PI) uptake and Annexin V-FITC fluorescence (data not shown), indicating less autophagy in apoptotic cells. Taken together, these results suggest a switch from autophagic repair to autophagy-driven apoptosis with prolonged exposure to nsPEF.

3.4. nsPEF activates early, mid, and late stage autophagy

In order to obtain a comprehensive view of the relationship between nsPEF exposure and autophagy activation, we examined protein expression of autophagy markers in response to pulsing. Beclin, an early marker of autophagy that is involved in phagopore formation, is increased at 50 and 100 pulses post-exposure in U937 and CHO-K1 cells (Fig. 4). Atg5 and Atg12, which bind together to form a complex during phagopore maturation, are also up-regulated at a low pulse number in U937 and CHO-K1 cells, although the response is stronger in CHO-K1 cells. Both cell lines

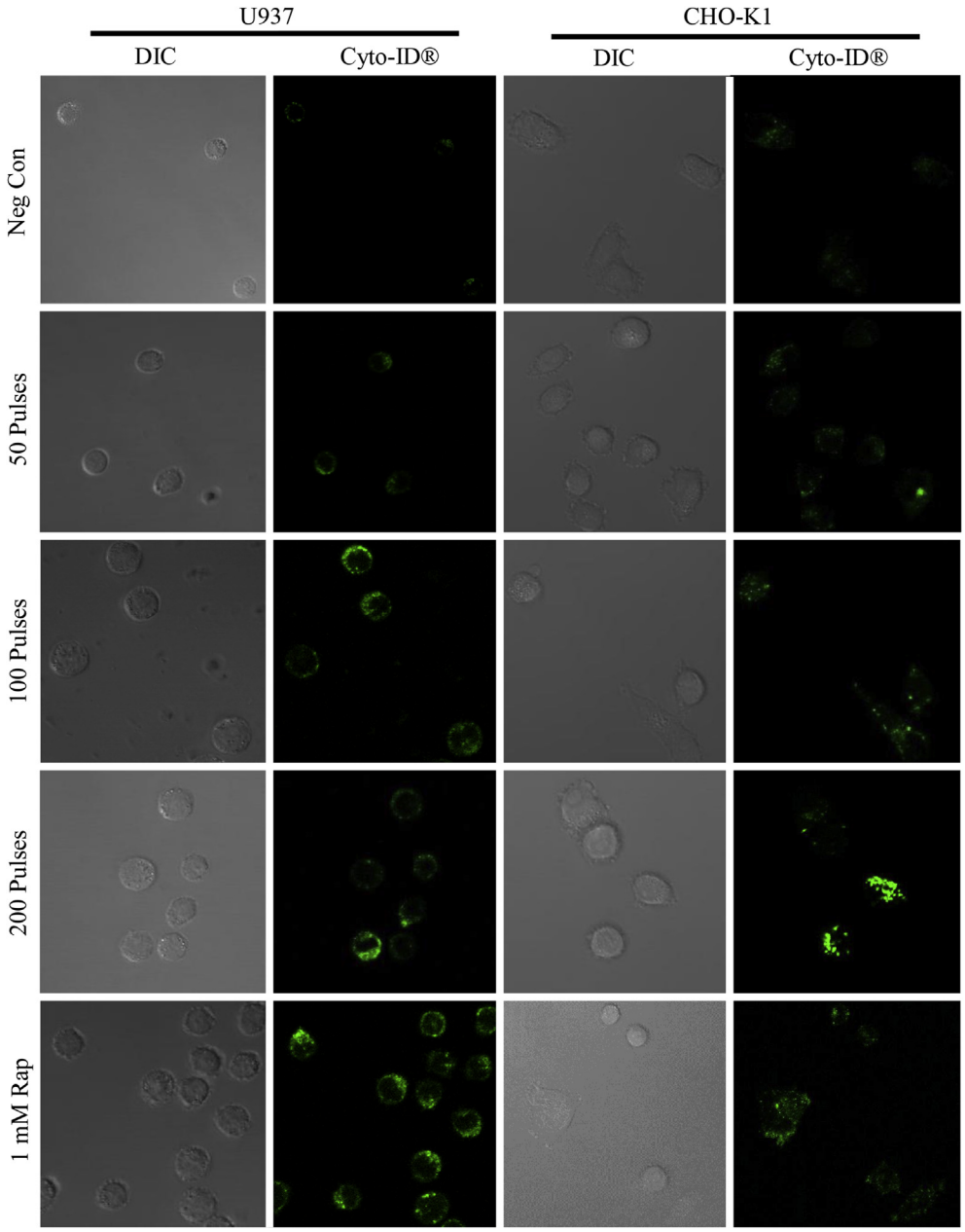

Fig. 3. Cyto-ID® immunofluorescence increases with prolonged nsPEF exposure, indicating activation of autophagy. Maximum Cyto-ID® staining is observed following 100 pulses (i.e., subtoxic exposure) in both U937 (left two columns) and CHO-K1 (right two columns). 1 mM rapamycin (rap) is included as a positive control (bottom row).

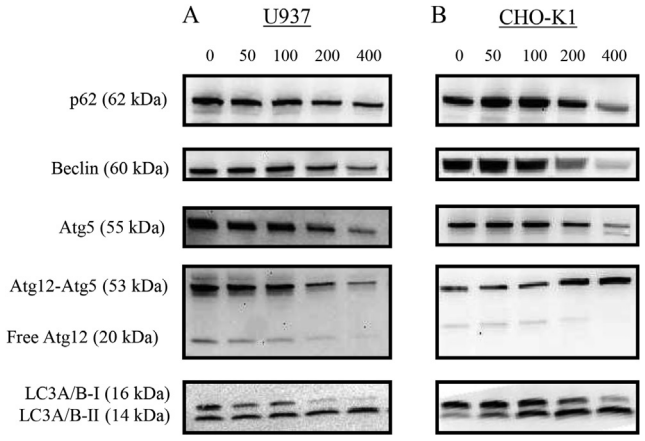

Fig. 4. nsPEF exposure induces changes in protein expression of various autophagy markers that are dependent on number of pulses. Results show Western blots of (A) U937 or (B) CHO-K1 cell lysates at various pulse numbers (0–400) at 4-h post-exposure. While the absolute expression of each marker varies, an overall trend is observed where the intensity of protein expression increases from 0 to 100 pulses, then drops dramatically with higher pulse number (>200 pulses).

exhibit increased Atg5-Atg12 complex, consistent with an early response to nsPEF (Fig. 4). As discussed above, LC3B is involved in the formation of autophagosomes. Importantly, LC3B isoform I undergoes post-translational modification to an active LC3B isoform II, which can associate with autophagic vesicles [22]. Accordingly, we observe a decrease in LC3B-I and a concomitant increase in LC3B-II with increasing pulse numbers, indicating activation of LC3B with nsPEF exposure (Fig. 4).

The absence of markers at higher pulse exposures suggests that autophagic membrane repair is not occurring under these conditions. One possible explanation for this observation is that longer exposures create extensive membrane damage that is beyond the cell's capacity to repair. This is evidenced by increased cell death at longer exposures (Fig. 1E). Supporting this explanation, p62 is downregulated at higher exposures (Fig. 1C–D). Thus, the combination of gene and protein expression data in concert with immunofluorescence establishes a timeline of autophagy, which is initially activated to repair nsPEF-induced damaged but becomes part of the mechanism of cell death.

4. Summary

The objective of the current study was to determine if autophagy is activated in cells following exposure to nsPEF. We demonstrate activation of autophagy following exposure to 50 or 100 pulses of 10 nsPEF (150 kv/cm) in two cell lines. Under these exposure conditions we see increased early (beclin), middle (Atg5, Atg12), and late (Cyto-ID®, p62, LC3B) stage autophagy markers, suggesting an active and complete autophagic process. In the present study, we hypothesized that autophagy was activated due to nsPEF-induced cellular damage. While the degree of plasma membrane damage induced by prolonged nsPEF exposure would be sufficient to activate repair mechanisms, it is possible that other effects of nsPEF exposure, such as reactive oxygen species generation, could activate autophagic machinery [23,24]. Additionally, nsPEF could damage lysosomes, rendering them unable to degrade material marked for autophagic repair. In support of this hypothesis, previous studies in our laboratory show disruption of lysosomal pathways following nsPEF [25]. Therefore, a large quantity of damaged cellular material and a reduced capacity of the lysosomes to recycle them could contribute to a switch to cell death mechanistic events as nsPEF exposure increase. Studies are currently in progress to address further the temporal activation and participation of these intracellular mechanisms during nsPEF exposure.

Conflict of interest

The authors declare no conflict of interest.

Acknowledgments

This research was supported by intramural funds from the Air Force Surgeon General's Office, Medical Research Program and the Air Force Office of Scientific Research LRIR 13RH08COR. Mr. Roth would like to thank the SMART program, grant number N002440910081 (OSO-T&E).

Transparency document

Transparency document related to this article can be found online at http://dx.doi.org/10.1016/j.bbrc.2015.01.131.

References

[1] A.M. Bowman, O.M. Nesin, O.N. Pakhomova, A.G. Pakhomov, Analysis of plasma membrane integrity by fluorescent detection of Tl(+) uptake, J. Membr. Biol. 236 (2010) 15–26.
[2] O.M. Nesin, O.N. Pakhomova, S. Xiao, A.G. Pakhomov, Manipulation of cell volume and membrane pore comparison following single cell permeabilization with 60- and 600-ns electric pulses, Biochim. Biophys. Acta 1808 (2011) 792–801.
[3] A.G. Pakhomov, J.F. Kolb, J.A. White, R.P. Joshi, S. Xiao, K.H. Schoenbach, Long-lasting plasma membrane permeabilization in mammalian cells by nanosecond pulsed electric field (nsPEF), Bioelectromagnetics 28 (2007) 655–663.
[4] P.T. Vernier, Y. Sun, M.A. Gundersen, Nanoelectropulse-driven membrane perturbation and small molecule permeabilization, BMC Cell Biol. 33 (2006) 37.
[5] M. Stacey, P. Fox, S. Buescher, J. Kolb, Nanosecond pulsed electric field induced cytoskeleton, nuclear membrane and telomere damage adversely impact cell survival, Bioelectrochemistry 82 (2011) 131–134.
[6] S.A. Curley, F. Palalon, X. Lu, N.V. Koshkina, Noninvasive radiofrequency treatment effect on mitochondria in pancreatic cancer cells, Cancer 120 (2014) 3418–3425.
[7] G.L. Thompson, C. Roth, G. Tolstykh, M. Kuipers, B.L. Ibey, Disruption of the actin cortex contributes to susceptibility of mammalian cells to nanosecond pulsed electric fields, Bioelectromagnetics 35 (2014) 262–272.
[8] A.G. Pakhomov, S. Xiao, O.N. Pakhomova, I. Semenov, M.A. Kuipers, B.L. Ibey, Disassembly of actin structures by nanosecond pulsed electric field is a downstream effect of cell swelling, Bioelectrochemistry 100 (2014) 88–95.
[9] D. Denton, T. Xu, S. Kumar, Autophagy as a pro-death pathway, Immunol. Cell Biol. 93 (2015) 35–42.
[10] S.A. Curley, F. Palalon, K.E. Sanders, N.V. Koshkina, The effects of non-invasive radiofrequency treatment and hyperthermia on malignant and nonmalignant cells, Int. J. Environ. Res. Public Health 11 (2014) 9142–9153.
[11] N.V. Koshkina, K. Briggs, F. Palalon, S.A. Curley, Autophagy and enhanced chemosensitivity in experimental pancreatic cancers induced by noninvasive radiofrequency field treatment, Cancer 120 (2014) 480–491.
[12] K. Liu, G. Zhang, Z. Wang, Y. Liu, J. Dong, X. Dong, J. Liu, J. Cao, L. Ao, S. Zhang, The protective effect of autophagy on mouse spermatocyte derived cells exposure to 1800 MHz radiofrequency electromagnetic radiation, Toxicol. Lett. 228 (2014) 216–224.
[13] B.L. Ibey, C.C. Roth, A.G. Pakhomov, J.A. Bernhard, G.J. Wilmink, O.N. Pakhomova, Dose-dependent thresholds of 10-ns electric pulse induced plasma membrane disruption and cytotoxicity in multiple cell lines, PLoS One 6 (2011) 1–11.
[14] M.H. Sahani, E. Itakura, N. Mizushima, Expression of the autophagy substrate SQSTM1/p62 is restored during prolonged starvation depending on transcriptional upregulation and autophagy-derived amino acids, Autophagy 10 (2014) 431–441.
[15] L. Zhou, H.F. Wang, H.G. Ren, D. Chen, F. Gao, Q.S. Hu, C. Fu, R.J. Xu, Z. Ying, G.H. Wang, Bcl-2-dependent upregulation of autophagy by sequestosome 1/p62 in vitro, Acta Pharmacol. Sin. 34 (2013) 651–656.
[16] S. Pankiv, T.H. Clausen, T. Lamark, A. Brech, J.A. Bruun, H. Outzen, A. Overvatn, G. Bjorkoy, T. Johansen, p62/SQSTM1 binds directly to Atg8/LC3 to facilitate degradation of ubiquitinated protein aggregates by autophagy, J. Biol. Chem. 282 (2007) 24131–24145.
[17] G. Bjorkoy, T. Lamark, A. Brech, H. Outzen, M. Perander, A. Overvatn, H. Stenmark, T. Johansen, p62/SQSTM1 forms protein aggregates degraded by

autophagy and has a protective effect on huntingtin-induced cell death, J. Cell. Biol. 171 (2005) 603–614.
[18] G. Bjorkoy, T. Lamark, S. Pankiv, A. Overvatn, A. Brech, T. Johansen, Monitoring autophagic degradation of p62/SQSTM1, Methods Enzymol. 452 (2009) 181–197.
[19] M. Lippai, P. Low, The role of the selective adaptor p62 and Ubiquitin-like proteins in autophagy, BioMed Res. Int. 2014 (2014) 11.
[20] J.P. Condreay, S.M. Witherspoon, W.C. Clay, T.A. Kost, Transient and stable gene expression in mammalian cells transduced with a recombinant baculovirus vector, Proc. Natl. Acad. Sci. 96 (1999) 127–132.
[21] L.L. Chan, D. Shen, A.R. Wilkinson, W. Patton, N. Lai, E. Chan, D. Kuksin, B. Lin, J. Qiu, A novel image-based cytometry method for autophagy detection in living cells, Autophagy 8 (2012) 1371–1382.
[22] Y. Kabeya, N. Mizushima, T. Ueno, A. Yamamoto, T. Kirisako, T. Noda, E. Kominami, Y. Ohsumi, T. Yoshimori, LC3, a mammalian homologue of yeast Apg8p, is localized in autophagosome membranes after processing, EMBO J 19 (2000) 5720–5728.
[23] C. Song, S.K. Mitter, H.V. Rao, J. Cai, X. Qi, M.E. Boulton, Oxidative stress-induced p62/SQSTM1 upregulation in the RPE, Invest. Ophthalmol. Vis. Sci. 53 (2012) 4765.
[24] O.N. Pakhomova, V.A. Khorokhorina, A.M. Bowman, R. Rodaitė-Riševičienė, G. Saulis, S. Xiao, A.G. Pakhomov, Oxidative effects of nanosecond pulsed electric field exposure in cells and cell-free media, Arch. Biochem. Biophys. 527 (2012) 55–64.
[25] G.L. Thompson, C.C. Roth, D.R. Dalzell, M. Kuipers, B.L. Ibey, Calcium influx affects intracellular transport and membrane repair following nanosecond pulsed electric field exposure, J. Biomed. Opt. 19 (2014) 055005.